

## Experimental and Analytical Computation of Forming Force, Major and Minor Strain and Its Validation by FEM in SPIF of UHMWPE

Manoj Prakash Bauskar<sup>1</sup>, Dr Prashant Singh<sup>2</sup>

<sup>1,2</sup>Bir Tikendrajit University, Manipur, India.

<sup>1</sup>AISSMSCOE, Pune, Maharashtra, India.

**Email ID:** mpbauskar@aissmscoe.com<sup>1</sup>, Prashant.singhkalhans@gmail.com<sup>2</sup>

### Abstract

Mass production is a fundamental requirement across various industries such as automotive, medical (e.g., artificial limbs), aerospace, and household appliances. Traditionally, this has been achieved through conventional metal forming processes like press work. However, for batch production scenarios, advanced and flexible manufacturing techniques such as Incremental Sheet Forming (ISF) are more suitable, as they can significantly reduce production costs. To optimize the ISF process, it is essential to study key process parameters, including step size, tool size, feed rate, spindle speed, and wall angle, as these factors directly influence formability and the deformation behavior particularly when working with Ultra High Molecular Weight Polyethylene (UHMWPE), which shows great potential in medical applications. This study aims to investigate critical aspects of the ISF process on UHMWPE, such as the forming limit diagram. It also involves a comparative analysis between experimental and analytical results using Finite Element Method (FEM), focusing major and minor strain values, and forming forces.

**Keywords:** FEM, Formability limit diagram, major & minor strain, DOE

### 1. Introduction

The Single Point Incremental Forming (SPIF) technique offers a major advantage by eliminating the need for dedicated punches or dies [1]. It operates by applying controlled plastic deformation to a sheet material, progressively forming it into the desired geometry. Due to the inherent flexibility of the Incremental Sheet Forming (ISF) process, it is well-suited for producing complex 3D shapes with a high level of customization [2,3]. In SPIF, the sheet is formed using a hemispherical tool (a single-point indenter) in conjunction with a fixture setup [4]. Among novel manufacturing techniques, ISF stands out for its capability to incrementally shape sheet metal using a CNC or VMC-controlled tool [5,6]. The absence of dedicated dies makes this process highly adaptable and cost-efficient, especially for low-volume production, prototyping, and custom manufacturing applications. In addition to experimental efforts, numerical simulations and behavioral studies of various sheet forming

processes, including stamping and incremental forming, play a critical role in understanding deformation behavior and optimizing process parameters [8,9]. This study specifically aims to investigate the Forming Limit Diagram (FLD) for Ultra High Molecular Weight Polyethylene (UHMWPE), as well as to compute forming forces, forming time, and major and minor strains—both experimentally and through Finite Element Method (FEM) analysis. Over the past few decades, the application of SPIF to polymeric materials has significantly increased. This growth is attributed not only to the method's inherent advantages but also to experimental observations demonstrating that SPIF can achieve strain levels beyond the conventional Forming Limit Curve (FLC) without inducing material failure [10–11]. Marques et al. [10] observed that polymer sheets often display delayed or completely suppressed necking, rendering the traditional FLC inadequate for characterizing their

formability. Instead, the Fracture Forming Line (FFL) is commonly used to define the formability limit of polymeric materials, taking into account their distinct deformation characteristics. In the context of SPIF applied to polymers with conical geometries, Martins et al. [12] identified three primary failure modes: circumferential cracking (cracks forming along the circumferential direction), twisting or wrinkling (resulting in material distortion and surface wrinkles), and oblique cracking (cracks developing along a bisector on the inclined wall). Of these, circumferential cracking and twisting are the most frequently observed. Le et al. [13] reported both failure types while forming cone-shaped parts with a circular arc generatrix from 3 mm thick polypropylene (PP) sheets. Similarly, Davarpanah et al. [14] investigated two SPIF geometries—one with a variable wall angle and another with a fixed-angle conical shape—using 0.7 mm thick polylactic acid (PLA) sheets, identifying similar failure patterns. Beyond these conventional failure modes, Rosa-Sainz et al. [15] uncovered an additional mechanism known as "crazing" in polycarbonate (PC) sheets subjected to SPIF.

## 2. Experimental Methodology

The Incremental Sheet Forming (ISF) tests were conducted using a FEELER VMP-40A Vertical Machining Center. Along with Fixture and Spherical tool. Taguchi L27 array is utilized for optimization of experiment. Tests were conducted on 1 mm-thick sheets of Ultra-High Molecular Weight Polyethylene (UHMWPE), a widely recognized biocompatible polymer. The experimental setup employed a conical frustum as the test geometry.

**Table 1 Experimental Input Parameters**

Parameters	Level 1	Level 2	Level 3
F: Feed (mm/min)	400	600	800
S: Spindle Speed(rpm)	400	600	800
D: Tool Diameter (mm)	8	10	12
Z: Step size(mm)	0.5	0.75	1



**Figure 1 Experimental Set Up**

### 2.1. Material Properties

The tensile test is carried out according to ASTM rectangular dog-bone shaped samples of the UHMWPE were performed to obtain the stress-strain curves [16]. Tests were done on Universal Testing Machine for plotting stress strain curve shown in (Figure 2)

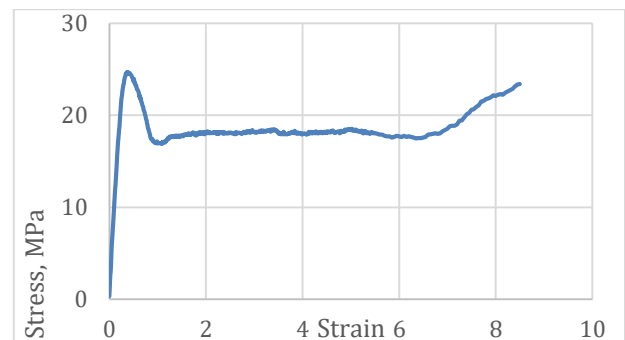


**Figure 2 Stress Strain Curve**

### 2.2. Finite Element Method

An explicit dynamic approach was used to simulate the SPIF process to produce a conical geometry with 50 ° angle, 30 mm depth, and 70 mm upper diameter with a tool, modelled as a rigid body, with hemispherical head of 12 mm in diameter and feed rate of 400 mm/s. The sheet metal was assumed to be UHMWPE. Both the sheet and the tool were simulated using shell elements by using following properties. Following step by step approach is used for simulation. First model is created in creo as per drawing then imported in Fusion 360 for generation of tool path first define stock 100 mm x100 mm in new set up for creating cone geometry. Then select spiral tool path and here defining tool as ball nose tool

by defining diameter of tool, Speed 600 rpm , feed 400 min/s. After this select forming area for actual forming and also define type of milling and step size 0.75 and movement of tool from outside to in. Do Post processing for creation of file to get position coordinates and file in the form of note pad is converted by G code ripper software in required csv type file for getting x,y and z co-ordinates. Then to

create position file for Abacus calculate total distance between x,y and z point also calculate time between two points by using following formula  $Velocity = \frac{Distance}{Time}$  by doing this will get total time for complete simulation. Now in Abaqus version 6.14.5 is used and following step by step approach is used as shown in Table 3 for analytical simulation.

**Table 2 Properties of FEM Part**

Part	Sheet	Tool
Material model	Mat Plasticity Polymer	3 D Rigid
Density[g/cm <sup>3</sup> ]	0.940	
Young Modulus [MPa]	114	
Poisson's Ratio	0.25	
Yield Stress[MPa]	16.9	
Ultimate Elongation	603	
Boundary condition	Rotational & translation constraint encastered along X,Y & Z translations for rigid part	
Contact conditions	Surface to Surface friction coefficient =0.05	

**Table 3 Approach for Simulation in Abacus**

Step	Process
1	Model creation of sheet 100*100 mm, 1 mm thick.
2	Tool modelling as rigid surface
3	Assembly and contact definition (friction=0.25, normal behaviour)
4	Material Property assignment defining Mesh size 1mmx1mm
5	Step definition: Time of analysis (from fusion)
6	Definition of displacement boundary condition for tool (displacement from fusion) & sheet (encastre).
7	Run the Job and Extract results.

mentioned Table 4. In the below figure 3a and 3b Major strain & Minor strain are calculated by FEM is shown. They agree well with each other as shown in (Table 4)

**Table 4 Comparison of Experimental & Analytical Major & Minor Strain**

Experiment Run 22	Major Strain	Minor Strain	% Error
Experimental Method	0.667	-0.287	Major Strain
			3.3
FEM	0.647	-0.313	Minor Strain
			8

### 3. Results and Discussion

#### 3.1.Comparison of Experimental & Analytical computed Major Strain and Minor Strain

Major and Minor Strain is computed for Run no 22 experimentally & analytical shown in below

#### 3.2.Comparison of Experimental & Analytical Computed Forming Force

Tool Force is computed for Run no 22 experimentally & analytical shown in below mentioned Table 5.

Which shows that Tool force computed analytically & experimentally agrees closely with each other.

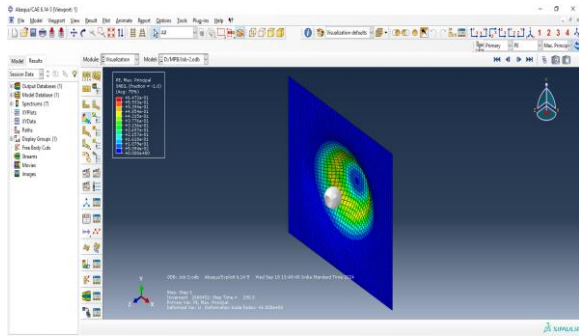


**Figure 3 Major Strain by Analytical Method**

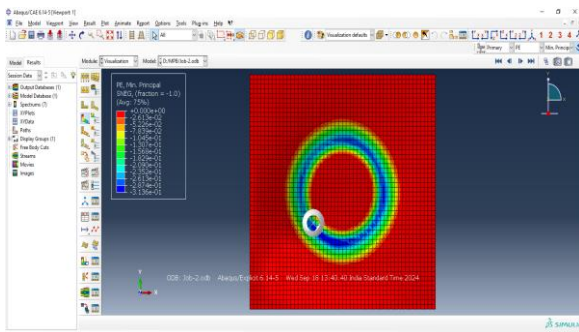


**Figure 4 Minor Strain by Analytical Method**

**Table 5 Comparison of Experimental & Analytical Forming Force**

Experiment Run 22	Forming Force N	% Error
Experimental Method	243	0.41
FEM	244	

Analytical result of forming force computed is shown in below (Figure 4)

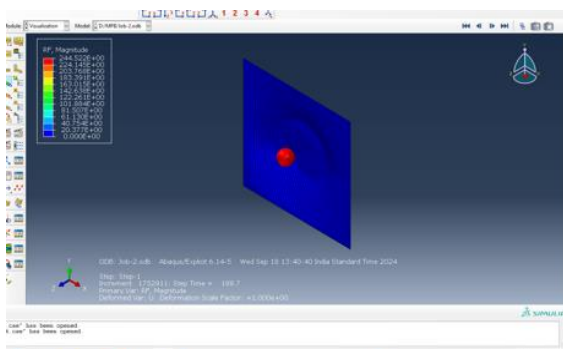


**Figure 5 Forming Force by Analytical Method**

### 3.3.Computation of Formability Limit Diagram by Experimental Method

Formability Limit diagram is constructed by generating grid of 5mm circle on sheet. After Incremental forming the dimensions of formed grid circle is measured and graph is plotted as shown in (Figure 6)

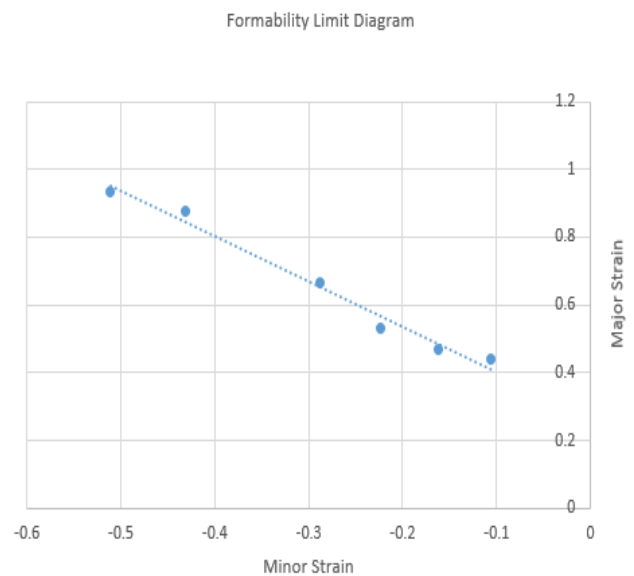


**Figure 5 Formability Limit Diagram**

### Conclusion

Strain: It is noted that Major and Minor strain computed by experimentally for run 22 and analytically (FEM) has Percentage deviation of 3.3% and 8% respectively. Forming Force: It is clear that the Tool force computed by experimental and Analytical (FEM) agrees well with each other. The Percentage deviation for Run 22 is 0.41%. Forming Limit Diagram: Forming Limit Diagram is successfully constructed for Single Incremental forming by plotting grid of Circle on given blank and after incremental forming process major and minor strain are computed.

### References

- [1]. Park J J, Kim Y H 2003 Fundamental studies on the incremental sheet metal forming technique J. Mater. Process. Technol. 140 447–453.
- [2]. Filice L, Fratini L, Micari F 2002 Analysis of material formability in incremental forming



- CIRP Ann. - Manuf. Technol. 51 199–202.
- [3]. Emmens W C, Sebastiani G, van den Boogaard A H 2010 The technology of Incremental Sheet Forming-A brief review of the history J. Mater. Process. Technol. 210 981–997.
  - [4]. Hagan E, Jeswiet J 2003 A review of conventional and modern single-point sheet metal forming methods Proc. Inst. Mech. Eng. Part B J. Eng. Manuf. 217 213–225.
  - [5]. Adams D, Jeswiet J 2015 Design rules and applications of single-point incremental forming Proc. Inst. Mech. Eng. Part B J. Eng. Manuf. 229 754–760.
  - [6]. Jeswiet J, Micari F, Hirt G, Bramley A, Dufloy J, Allwood J 2005 Asymmetric Single Point Incremental Forming of Sheet Metal CIRP Ann. - Manuf. Technol. 54 88–114.
  - [7]. Kim H, Park T, Esmailpour R and Pourboghrat F 2018 Numerical Study of Incremental Sheet Forming Processes J. Physics: Conf. Series. 1063 012017.
  - [8]. Mohammed B, Park T, Pourboghrat F, Hu J, Esmailpour R and Abu-farha F 2017 Multiscale crystal plasticity modeling of multiphase advanced high strength steel strength steel Int. J. Solids and Structures.000 1–19.
  - [9]. Marques, T.A.; Silva, M.B.; Martins, P.A.F. On the Potential of Single Point Incremental Forming of Sheet Polymer Parts. Int. J. Adv. Manuf. Technol. 2012, 60, 75–86.
  - [10]. Centeno, G.; Morales-Palma, D.; Gonzalez-Perez-Somarriba, B.; Bagudanch, I.; Egea-Guerrero, J.J.; Gonzalez-Perez, L.M.; García Romeu, M.L.; Vallellano, C. A Functional Methodology on the Manufacturing of Customized Polymeric Cranial Prostheses from CATUsing SPIF. Rapid Prototyp. J. 2017, 23, 771–780.
  - [11]. Martins, P.A.F.; Kwiatkowski, L.; Franzen, V.; Tekkaya, A.E.; Kleiner, M. Single Point Incremental Forming of Polymers. CIRP Ann. Manuf. Technol. 2009, 58, 229–232.
  - [12]. Le, V.S.; Ghiotti, A.; Lucchetta, G. Preliminary Studies on Single Point Incremental Forming for Thermoplastic Materials. Int. J. Mater. Form. 2008, 1, 1179–1182.
  - [13]. Davarpanah, M.A.; Mirkouei, A.; Yu, X.; Malhotra, R.; Pilla, S. Effects of Incremental Depth and Tool Rotation on Failure Modes and Microstructural Properties in Single Point Incremental Forming of Polymers. J. Mater. Process. Technol. 2015, 222, 287–300.
  - [14]. Rosa-Sainz, A.; Centeno, G.; Silva, M.B.; Vallellano, C. Experimental Failure Analysis in Polycarbonate Sheet Deformed by Spif. J. Manuf. Process. 2021, 64, 1153–1168.
  - [15]. Esmailpour R, Kim H, Park T, Pourboghrat F, Xu Z, Mohammed B and Abu-Farha F 2018 Calibration of Barlat Yld2004-18P Yield Function Using CPFEM and 3D RVE for the Simulation of Single Point Incremental Forming (SPIF) of 7075-O Aluminum Sheet Int. J. Mech. Sci. 145 24–41.